*photonics*

MDPI

*Article*

# Biofunctionalized Polyelectrolyte Microcapsules Encoded with Fluorescent Semiconductor Nanocrystals for Highly Specific Targeting and Imaging of Cancer Cells †

**Galina Nifontova [1], Daria Kalenichenko [1,2], Maria Baryshnikova [3], Fernanda Ramos Gomes [4], Frauke Alves [4,5], Alexander Karaulov [6], Igor Nabiev [1,2,6,*] and Alyona Sukhanova [2,*]**

1 Laboratory of Nano-Bioengineering, National Research Nuclear University MEPhI (Moscow Engineering Physics Institute), 31 Kashirskoe shosse, Moscow 115409, Russian
2 Laboratoire de Recherche en Nanosciences, LRN-EA4682, Universite de Reims Champagne-Ardenne, 51 rue Cognacq Jay, Reims 51096, France
3 N.N. Blokhin National Medical Research Center of Oncology, 23 Kashirskoe shosse, Moscow 115478, Russian
4 Translational Molecular Imaging, Max-Planck-Institute of Experimental Medicine, 3 Hermann-Rein-Str., Göttingen 37075, Germany
5 Clinic of Haematology and Medical Oncology, University Medical Center Göttingen, 40 Robert-Koch-Str., Göttingen 37075, Germany
6 Department of Clinical Immunology and Allergology, I.M. Sechenov First Moscow State Medical University, Moscow 119992, Russian
* Correspondence: igor.nabiev@univ-reims.fr (I.N.); alyona.sukhanova@univ-reims.fr (A.S.); Tel.: +33-6-3125-9180 (I.N.)
† This paper is an extended version of Nifontova, G.; Baryshnikova, M.; Ramos Gomes, F.; Alves, F.; Nabiev, I.; Sukhanova, A. Engineering of fluorescent biomaging tools for cancer cell targeting based on polyelectrolyte microcapsules encoded with quantum dots. In Proceedings of the 4th International Conference on Applications of Optics and Photonics, AOP2019, Lisbon, Portugal, 31 May–1 June 2019.

Received: 25 September 2019; Accepted: 5 November 2019; Published: 8 November 2019


**Abstract:** Fluorescent semiconductor nanocrystals or quantum dots (QDs) are characterized by unique optical properties, including a high photostability, wide absorption spectrum, and narrow, symmetric fluorescence spectrum. This makes them attractive fluorescent nanolabels for the optical encoding of microcarriers intended for targeted drug delivery, diagnosis, and imaging of transport processes on the body, cellular, and subcellular levels. Incorporation of QDs into carriers in the form of polyelectrolyte microcapsules through layer-by-layer adsorption of oppositely charged polyelectrolyte polymers yields microcapsules with a bright fluorescence signal and adaptable size, structure, and surface characteristics without using organic solvents. The easily modifiable surface of the microcapsules allows for its subsequent functionalization with capture molecules, such as antibodies, which ensures specific and selective interaction with cells, including tumor cells, with the use of the bioconjugation technique developed here. We obtained stable water-soluble nanolabels based on QDs whose surface was modified with polyethylene glycol (PEG) derivatives and determined their colloidal and optical characteristics. The obtained nanocrystals were used to encode polyelectrolyte microcapsules optically. The microcapsule surface was modified with humanized monoclonal antibodies (Abs) recognizing a cancer marker, epidermal growth factor receptor (EGFR). The possibility of effective, specific, and selective delivery of the microcapsules to tumor cells expressing EGFR has been demonstrated. The results show that the QD-encoded polyelectrolyte microcapsules functionalized with monoclonal Abs against EGFR can be used for targeted imaging and diagnosis.

**Keywords:** quantum dots; fluorescent imaging; fluorescent nanolabels; polyelectrolyte microcapsules; antibody-mediated targeted delivery

## 1. Introduction

Methods of fluorescence imaging are used to analyze transport, distribution, and interaction processes on the molecular, cellular, and tissue levels. A high sensitivity, the possibility of real-time analysis, non-invasiveness, and safety of recording the signal make fluorescence imaging highly demanded in diagnostic methods and in tracing the transport of drugs and vehicles for their delivery to specific cells or body compartments. For the imaging to be possible, the drugs or systems of their delivery should be fluorescent, which, if they have no inherent fluorescence, can be ensured by tagging them with fluorophores characterized by distinct, bright, and stable fluorescence [1,2]. The role of such fluorescent tags can be played by fluorescent semiconductor nanocrystals referred to as quantum dots (QDs). QDs possess unique optical properties, including high fluorescence quantum yield and molar extinction coefficient, a wide absorption spectrum, and a narrow, symmetric emission spectrum with the peak wavelength determined by the physical size of the nanocrystal [3]. Resistance to photobleaching and photo- and chemically induced destruction makes QDs more attractive labels than the organic molecules routinely used for this purpose in bioimaging and fluorescent detection. The QDs to be used as nanolabels in biomedical applications should be soluble in water and biological fluids, colloidally stable, and biocompatible [4,5]. The optimal characteristics of QDs can be ensured by replacing their original surface ligands with water-soluble ones (mercaptopropionic acid, cysteamine, cysteine, etc.), as well as by solubilizing them with stabilizing hydrophilic ligands, such as thiol-containing surfactants. However, colloidal characteristics of QDs, such as their size, shape, surface charge, and surface ligand composition, determine their potential toxicity, which limits the use of QDs in biomedicine [6].

Micro- and nanosized carriers can be fluorescently labeled or optically encoded through the incorporation of QDs into them [7,8]. In this case, the shell of the carrier serves as a barrier restricting the interaction of QDs with biological structures, which increases their general biocompatibility. Polyelectrolyte microcapsules are promising carriers for various agents, such as fluorescent labels, fluorescently tagged polymers, nucleic acids, peptides, proteins, drugs, and nanoparticles (plasmonic, magnetic, and fluorescent semiconductor ones) that can be placed (encapsulated) into them [9]. Polyelectrolyte microcapsules are obtained by means of layer-by-layer adsorption of oppositely charged polyelectrolytes onto the surface of microparticles with a matrix structure, which results in core/shell microcapsules. Soft-shell microcapsules are obtained through subsequent removal of the core with the use of specific agents that do not disturb the integrity of the polyelectrolyte shell coating the core [10]. Microcapsules with a soft structure have enough flexibility to move into zones characterized by enhanced penetrability (such as inflammation and tumor growth zones). In addition, the technology of layer-by-layer application of polyelectrolytes makes it possible to use preliminarily functionalized cores, as well as to embed functional components into the polymer shell while it is formed. This can be used to separate different functional components from one another within the carrier structure to cope with their chemical, physical, or pharmacological incompatibility. The surface of the microcapsules can be modified with various ligands, including capture molecules, e.g., antibodies (Abs) against specific receptors of tumor cells (cancer markers). Thus, the microcapsules can be functionalized via bioconjugation and, hence, used for targeted delivery to tumor cells [11,12].

Epidermal growth factor receptor (EGFR) characterized by inherent tyrosine kinase activity, which controls cell proliferation is expressed by many tumors, such as head, neck, ovary, bladder, and esophagus cancers, and is the key marker for their diagnosis and targeted therapy [13–15].

The goal of this study was to develop approaches to obtaining water-soluble, colloidally stable core/shell QDs with the use of polyethylene glycol (PEG) derivatives containing thiol and carboxyl-terminal functional groups, as well as to design polyelectrolyte microcapsules fluorescently

tagged with QDs as nanolabels. We also report the optical and dispersion characteristics of both QDs and QD-encoded microcapsules fabricated in this study, as well as the results of studying the possibility for targeted delivery of the microcapsules to tumor cells, in particular, those expressing the cancer marker EGFR, after vectorization with humanized monoclonal anti-EGFR Abs (Cetuximab, Erbitux®) used for treatment of EGFR-positive tumors. Our data demonstrate that the QD-encoded polyelectrolyte microcapsules can serve as a basis for designing theranostic and fluorescent agents for targeted drug delivery, detection of tumor cells, and tracking of transport processes.

## 2. Materials and Methods

### *2.1. Obtaining Water-Soluble, Colloidally Stable Quantum Dots*

CdSe/ZnS core/shell QDs with a fluorescence peak wavelength of 600 nm, coated with trioctylphosphine oxide (TOPO) were kindly provided by Dr. Pavel Samokhvalov (LNBE, NRNU MEPhI, Moscow, Russian Federation). The QDs were initially purified from excess of TOPO by a series of dissolution/precipitation cycles in a chloroform-methanol mixture. Then, the QDs were transferred to the aqueous phase by replacing the TOPO ligand with DL-cysteine. The water-soluble QDs were additionally solubilized with a PEG derivative containing sulfhydryl and carboxyl end groups ($CT(PEG)_{12}$, Thermo Scientific, Rockford, Illinois, USA) as described earlier [16]. The water-soluble QDs stabilized with the PEG derivative were purified from the unbound ligands using gel filtration. The optical properties of the obtained QD samples were estimated by means of an Agilent Cary 60 spectrophotometer and an Agilent Cary Eclipse spectrofluorometer. The QD hydrodynamic diameter and surface charge were analyzed by the dynamic light scattering and laser Doppler electrophoresis methods using a Zetasizer Nano ZS (Malvern, Worcestershire, UK).

### *2.2. Synthesis of Polyelectrolyte Microcapsules Encoded with Quantum Dots*

Polyelectrolyte microcapsules were obtained through layer-by-layer adsorption of oppositely charged polyelectrolytes, the polycation poly(allylamine hydrochloride) (PAH, 15,000 Da) and the polyanions poly(styrenesulfonate sodium salt) (PSS, 70,000 Da), polyacrylic acid (PAA, 15,000 Da). The polymers were purchased from Sigma-Aldrich (USA). The polyelectrolytes were applied onto the surface of calcium carbonate microparticles used as a substrate. These microparticles were obtained by the precipitation method with the use of equimolar calcium chloride and sodium carbonate solutions at a ratio of 1:1 (v/v). Initially, the template particles were dispersed in 0.5 mL of ultrapure water. Then, 0.5 mL of a 2 mg/mL polyelectrolyte solution in 0.5 M NaCl was added to 0.5 mL of a suspension. The polyelectrolytes were applied onto the substrate in the following order: PAH/PSS/PAH/PSS/PAH/PSS/PAH/PSS/PAH/PSS. After deposition of each polyelectrolyte, the excess of the polymer was washed by centrifugation using ultrapure water.

The microcapsules were labelled with the prepared water-soluble QDs via adsorption of the QDs onto the calcium carbonate microparticles preliminarily coated with the PAH/PSS/PAH/PSS/PAH layers as described elsewhere [17,18]. The layer of adsorbed QDs was then coated with additional polyelectrolyte layers in the order PAH/PSS/PAH/PSS/PAH/PSS. The sizes and fluorescence characteristics of the resultant microparticles were analyzed using optical and fluorescence microscopies.

### *2.3. Obtaining Microcapsules with a Hollow Structure Not Containing the Substrate*

The microcapsules with a hollow structure not containing the substrate were obtained by dissolving the microparticles in 0.5 M sodium ethylenediaminetetraacetate (EDTA) (Sigma-Aldrich, USA) solution (pH 8.0). The microcapsules used had the following structure: $CaCO_3$/PAH/PSS/PAH/PSS/PAH/PSS/PAH/PSS/PAH/PSS. Specifically, $6 \times 10^6$ microcapsules containing cores were resuspended in 5 ml of 0.5 M EDTA (pH 8.0) and incubated for 2, 4, 8, 16, and 32 h at room temperature while stirring. After the incubation, the obtained microcapsules were sedimented by centrifugation; the, supernatant was withdrawn and replaced with purified water. The washing off of

the products of the core dissolution was repeated three times. After the last washing, the microcapsules were resuspended in 0.5 ml of MilliQ water.

In order to determine how completely the template was removed and estimate the permeability of the polyelectrolyte shell, the soft microcapsules were stained with dyes of different molecular weights (trypan blue with Mw 960.8 g/mol). $6 \times 10^6$ microcapsules were resuspended in 0.5 ml of 0.05 M phosphate buffer (pH 8.0) containing 2.3 mM of trypan blue. The samples were incubated on a rotary shaker for 16 h at 25 °C and thermostatic conditions. After the incubation, the staining efficiency of the microcapsules was analyzed. The quantity of the dye entrapped within the microcapsules was estimated spectrophotometrically using a SPARK10M multimodal plate reader (Tecan, Switzerland).

### *2.4. Bioconjugation of the Quantum Dot–Encoded Polyelectrolyte Microcapsules with Monoclonal Antibodies*

Before bioconjugation of the microcapsules, their surface was coated with PAA, and the calcium carbonate template was removed using EDTA. Then the surface of the microcapsules was activated by means of the carbodiimide reaction involving 1-ethyl-3-(3-dimethylaminopropyl)-carbodiimide hydrochloride (EDC) (Thermo Fisher Scientific, USA) and N-hydroxysulfosuccinimide (sulfo-NHS) (Thermo Fisher Scientific, Rockford, Illinois, USA). Different amounts of humanized monoclonal anti-EGFR Abs (Cetuximab, Erbitux® from Merck Serono, Germany) were loaded to functionalize the microcapsules. The biofunctionalization was performed for 2 h at room temperature with the use of a zero-length carbodiimide cross-linker as described earlier [19]. Briefly, 10 µL of 50 mg/mL sulfo-NHS and EDC were subsequently added to the $6 \times 10^6$ of PAA-coated hollow QD-encoded microcapsules. The pre-activated microcapsules were washed off the excess of cross-linkers with 50 mM phosphate buffer (pH 7.2) via centrifugation. Then, the monoclonal anti-EGFR Abs were added to the microcapsule suspension, and the volume of the reaction mixture was adjusted to 0.5 mL. The suspension was mixed while shaking for 2 h at room temperature in the absence of light. After that, the microcapsules were washed with 10 mM PBS (pH 7.4) by centrifugation and resuspended in 10 mM PBS (pH 7.4) containing 1% of bovine serum albumin (BSA). The effectiveness of the surface functionalization was estimated as the ratio between the amount of Abs bound to the microcapsule surface and the initial Ab content of the reaction mixture. The amount of bound Abs was determined as the difference between the Ab content in the mixture before and after the reaction, which were measured spectrophotometrically using a NanoDrop 2000 (Thermo Fischer, Rockford, Illinois, USA). The surface charge of the resultant conjugates was measured using a Zetasizer Nano ZS (Malvern Instruments, Worcestershire, UK).

### *2.5. Assessment of the Possibility to Target Tumor Cells with the Quantum Dot–Encoded Polyelectrolyte Microcapsules Functionalized with Monoclonal Antibodies*

The functional activity of the obtained polyelectrolyte microcapsules containing QDs and carrying monoclonal anti-EGFR Abs on the surface were estimated in experiments on cultured cells. MDA-MB-468 human breast adenocarcinoma cells were used as model EGFR-expressing tumor cells, and MCF-7 cells served as EGFR-negative control cells. The cells were plated onto four-chamber slides and cultured at 37 °C for 12 h. Then, $6 \times 10^6$ fluorescent polyelectrolyte microcapsules conjugated with monoclonal anti-EGFR Abs and additionally treated with BSA were suspended in the supplemented culture medium and added to the cell culture. The microcapsule-cell interaction was analyzed using an SP5 confocal laser scanning microscope (Leica Microsystems, Germany) as described earlier [17]. The fluorescence signal of the functionalized, QD-encoded microcapsules was recorded in the wavelength range from 550 to 653 nm, with the fluorescence excited at 488 nm. In confocal images, the particle number was estimated by means of a particle counting mask during post-processing using the Fiji software (an image processing package based on ImageJ software, USA).

## 3. Results and Discussion

### *3.1. Design and Preparation of Quantum Dot-Encoded Polyelectrolyte Microcapsules*

The prepared template calcium carbonate microparticles were 4.0 to 6.0 μm in size and were characterized with a slightly negative ζ-potential (− 6.0 ± 1.6 mV), enabling the application of the polycation PAH as the first polyelectrolyte layer that facilitated primary polymer layer deposition by electrostatically driven adsorption. Then, the polyelectrolyte shell was formed by depositing a polyanion (the negatively charged PSS) and subsequently alternating the PAH and PSS layers until the desired shell thickness was reached.

The resultant water-soluble QDs, after the purification, ligand exchange, and solubilization, had typical wide adsorption and narrow symmetrical fluorescence spectra, the position of the fluorescence maximum remaining the same (600 nm) as demonstrated in Figure S1, Supplementary Materials. The QDs had a hydrodynamic diameter ranging from 19.2 to 24.3 nm (Figure S1, Supplementary Materials) and a ζ-potential of –33.2 ± 1.2 mV, ensuring their effective entrapment within the positively charged polyelectrolyte layers of the microcapsule shell.

A single layer of QDs was applied onto the PAH-coated microparticles, and then the QDs were immobilized with outer polyelectrolyte layers (Figure 1a). Each cycle of polyelectrolyte and QD deposition was characterized by flips in the surface charge of the microparticles, which varied from −26 mV to +15 mV. Flips of surface charges by layer-by-layer coating were examined by zeta-potential measurements using a ZetaSizer Nano ZS (Malvern Instruments, Worcestershire, UK) and were presented in our previous studies [17,18]. The resultant microcapsules were characterized by the size and shape similar to those of the template microbeads used. The microphotograph of the QD-encoded microcapsules demonstrates their bright fluorescence determined by the QDs (Figure 1b). The QD localization pattern within the polyelectrolyte shell was already investigated in microcapsule sections using fluorescence microscopy, where the highly homogeneous distribution of QDs fluorescence within the shell was observed [18]. The loading of QDs on microparticles was quantified earlier [17]. For the microcapsule surface area of nearly $8.2 \times 10^7$ nm$^2$, the total surface area of the deposited QDs was found to be ~$4.6 \times 10^9$ nm$^2$. This fact shows a multilayer character of QD adsorption during their layer-by-layer deposition on the microcapsule surface. The fluorescence properties of the final microparticles, including the fluorescence spectra and lifetimes of embedded QDs, have been examined and described in our previous studies [17,18].

After that, the surface of the microcapsules was modified with different polymers containing the functional groups required for bioconjugation (e.g., PAA and PAH), and the calcium carbonate microparticles were dissolved to obtain hollow fluorescent microcapsules.

Hollow-structured polyelectrolyte microcapsules were obtained using EDTA as a calcium-specific dissolution agent, preserving the interpolymer complex deposited on the template cores [20]. Since the microcapsule polyelectrolyte shell is supposed to be permeable for low-molecular-weight compounds, EDTA (Mw 372.2 g/mol) and its water-soluble complexes with calcium ions forming during interaction with calcium carbonate template are expected to be removed out of the microcapsules due to the penetration through the polyelectrolyte shell. To analyze the permeability of the designed shell for the low-molecular-weight compounds, EDTA-treated microcapsules were stained with a low-molecular-weight dye such as trypan blue. The obtained results showed effective entrapment of the dye within the microcapsules of the designed shell thickness (Figure 2). All the microcapsule samples after treatment with 0.5 M EDTA (pH 8.0) preserved the integrity of their shells, indicating the possibility of the usage of such agents even for long-term treatment of microcapsules. The highest entrapment efficiencies of trypan blue were achieved after 6 h of the templated microcapsules treatment with EDTA. This could be explained by a higher molecular weight of the dye comparing to that of EDTA and its calcium complexes, ensuring slower diffusion of trypan blue into the microcapsules, particularly at the initial time points during core removal. The residuals of calcium carbonate microparticles possibly remaining inside the microcapsule shell during short-term template dissolution could have

acted as a barrier for the dye penetration [21,22]. However, after longer incubation of the templated microcapsules in the EDTA solution, a moderate decrease in trypan blue entrapment efficiency was observed. This was likely a result of effective core dissolution that probably led to the acceleration in mass-transfer of the dye through the polyelectrolyte shell, as well as in its diffusion out of the microcapsule interior.

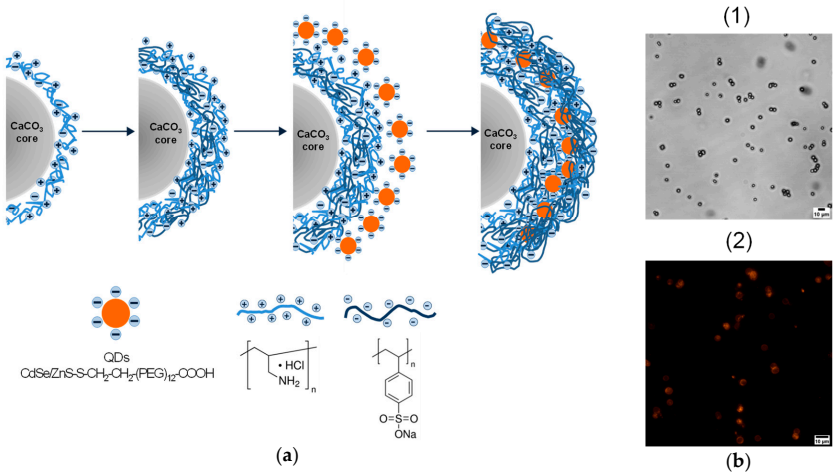


**Figure 1.** Polyelectrolyte shell formation and optical encoding with quantum dots (QDs) using a layer-by-layer deposition: (**a**) the scheme of the polyelectrolyte and QD deposition onto the calcium carbonate microparticle surface; (**b**) microphotographs of the synthesized calcium carbonate template microparticles (1) and resultant QD-encoded microcapsules (2). The fluorescent image was obtained using an XF115-2 FITC long pass filter set consisting of a 505DRLP dichroic filter, a 475AF40 excitation filter, and a 510ALP emission filter.

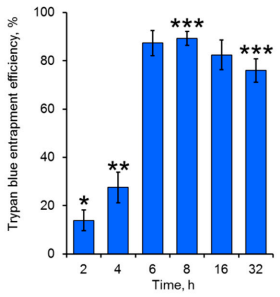


**Figure 2.** Efficiency of the microcapsule staining using trypan blue: * the data are significantly different from 4, 6, 8, 16, 32 h ($p < 0.05$); ** the data are significantly different from 6, 8, 16, 32 h ($p < 0.05$); *** the data are significantly different from 8 and 32 h ($p < 0.05$).

### 3.2. *Functionalization of the Quantum Dot-Encoded Polyelectrolyte Microcapsules with Monoclonal Antibodies*

Prior to the functionalization of the microcapsules, their surface was treated with PAA to ensure the exposure of free carboxyl groups and subsequent chemical surface activation and bioconjugation. Immediately after PAA adsorption, the calcium carbonate template was removed.

Functionalization of the microcapsules was performed using covalent coupling, which is known to be a stronger and more effective way of Ab immobilization compared to passive adsorption. The EDC and sulfo-NHS crosslinkers were used for the activation of the carboxyl groups constituting the outer layer of the polyelectrolyte shell. EDC interaction with sulfo-NHS during the activation step resulted in the formation of the sulfo-NHS–ester intermediate which is reactive towards the primary amino groups of Ab, forming a covalent amine bond as shown in Figure 3a.

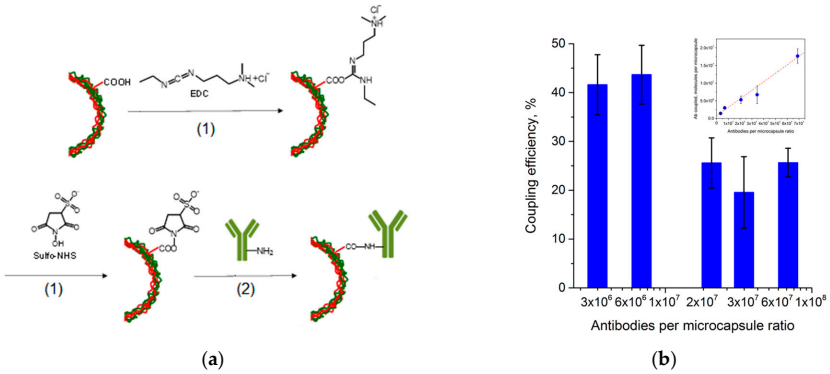


**Figure 3.** Coupling of antibodies to the microcapsule surface: (**a**) the scheme of the microcapsule surface activation (1) and antibody coupling (2); (**b**) antibody coupling efficiency, the data on the coupling yield are presented in the inset.

The Ab coupling was performed in excess of humanized monoclonal anti-EGFR Abs using the following microcapsule to Ab molecule ratios: 1:($3 \times 10^6$), 1:($7 \times 10^6$), 1:($2 \times 10^7$), 1:($3 \times 10^7$), and 1:($7 \times 10^7$). The quantity of the Abs involved in the conjugation was estimated, and the coupling efficiencies were determined. The obtained results are presented in Figure 3b and demonstrate enrichment of the microcapsule surface with coupled Abs with increasing Ab content in the mixture. However, a higher coupling efficiency was obtained at lower microcapsule to Ab molecule ratios. Higher microcapsule to Ab molecule ratios led to a decrease in the Ab coupling rate, possibly explained by saturation of the microcapsule surface with Abs and lack of available active sites for Ab attachment. The resultant bioconjugates of the fluorescent QD-encoded microcapsules and anti-EGFR Abs were characterized by the size distribution similar to that of the original nanolabelled microcapsules, the particle diameter varying from 4.0 to 6.1 μm. The prepared Ab-functionalized, QD-encoded microcapsules preserved their dispersion state; the crosslinker surface activation did not cause aggregation of the microcapsules. To finalize the coupling procedure, the microcapsules were isolated from the reaction mixture and washed from the excess reactants. To block the active sites free of Abs on the microcapsule surface, they were back-coated with BSA. The average surface charge of the resultant Ab-functionalized microcapsules was estimated as −14.2 ± 2.6 mV.

### *3.3. Cancer Cell Targeting Activity of the Designed Microcapsules*

Here, our goal was to perform primary analysis of microparticle–cell interaction in terms of cancer cell recognition and targeting against cell membrane receptors, in particular, EGFR. Testing of the functional activity of the designed Ab-functionalized, QD-encoded microcapsules was performed using live cells expressing EGFR, namely, MDA-MB-468 human breast adenocarcinoma cells. The possibility of nonspecific interaction was studied using similar human breast adenocarcinoma cells, MCF-7, which did not express EGFR and were used as an EGFR-negative control. The interaction was analyzed during 1 h after the microcapsule samples were added to both types of cells.

We used the QD-encoded microcapsules conjugated with humanized monoclonal anti-EGFR Abs at a ratio of 1:($2 \times 10^7$), which we considered the most promising in terms of the Ab content and coupling efficiency. The data shown in Figure 4 demonstrate the interaction of the Ab-functionalized microcapsules with the live EGFR-positive MDA-MB-468 cells. The microcapsules were observed to be located all over the cell surface (Figure 5a), exhibiting their efficiency in targeting the MDA-MB-468 cells. The amount of the microcapsules attached to the cells varied from 1 to 9, depending on the cell size and availability for particle attachment. However, the contribution of nonspecific interaction had to be analyzed. For that purpose, we prepared samples of BSA-coated microcapsules without Abs. BSA was used as a back-coating agent in bioconjugation to block activated areas of the microcapsule surface and make it more inert to the microenvironment and more biocompatible [18].

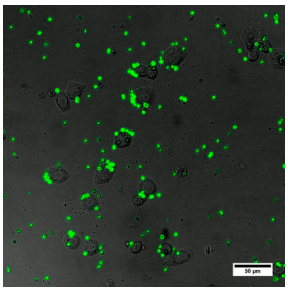

**Figure 4.** General view of the MDA-MB-468 human breast adenocarcinoma cells interacting with the antibody-functionalized, quantum dot-encoded microcapsules.

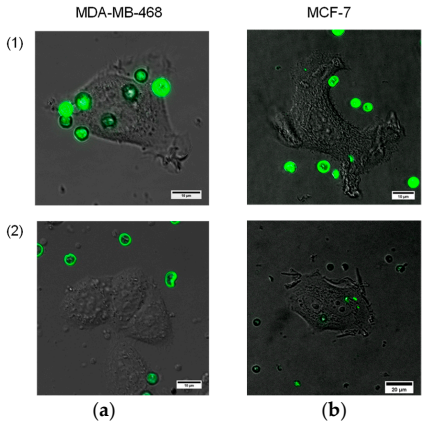


**Figure 5.** Images of individual cancer cells or their groups interacting with the QD-encoded microcapsules ((1) antibody-functionalized microcapsules; (2) bovine serum albumin-coated microcapsules): (**a**) MDA-MB-468 human breast adenocarcinoma cells; (**b**) MCF-7 human breast adenocarcinoma cells.

As shown in Figure 5, the interaction of the conjugates with EGFR-negative cells was almost negligible. BSA-coated control samples of the QD-encoded microcapsules revealed no distinct binding to either EGFR-positive or EGFR-negative cells, which indicates the specificity of the interaction of the conjugated microcapsules with cells and demonstrates their functional activity in terms of live cancer cell targeting. In the present study, the cancer cell targeting capacity, in particular, the specific interaction of the particles with the cell membrane receptors (in terms of proof-of-concept studies of the designed antibody-functionalized QD-encoded microcapsules) was investigated. However, it is known that macropinocytosis and phagocytosis involving lipid raft formation are typically involved in the uptake of polyelectrolyte microcapsules [23]. Earlier, the QD-encoded microcapsule uptake by murine alveolar macrophages was studied [17], and the primary signs of lipid raft formation have been observed. The analysis of the internalization pathways and intracellular localization of the microcapsules has to be investigated and will be further considered.

## 4. Conclusions

In this study, we have described an approach for the fabrication of hollow-structured polyelectrolyte microcapsules and their optical encoding with stable water-soluble QDs. The effectivity of calcium carbonate cores used as templates for polyelectrolyte deposition was confirmed by staining of the resultant hollow microcapsules with trypan blue dye, which demonstrated the possibility of further spontaneous, diffusion-driven drug loading of low-molecular-weight compounds with similar molecular weights, e.g., doxorubicin as an anti-cancer agent, into the designed microcapsules. The obtained QD-labelled microcapsules are characterized by optimal size distribution, dispersion state and, sufficient fluorescent signal to be detectable by fluorescence microscopy techniques. The designed

fluorescent polyelectrolyte microcapsules have been successfully functionalized with monoclonal Abs (cetuximab), providing effective targeting of the particles to cancer cells. The engineered bioconjugates of the microcapsules and Abs exhibit particle–cell interaction specificity, which has been demonstrated using an EGFR-expressing cancer cell model. Thus, the designed QD-encoded polyelectrolyte microcapsules are a promising platform for biofunctionalization and cancer cell targeting in further developing of novel, sophisticated fluorescent bioimaging and theranostic tools.

**Supplementary Materials:** The following are available online at http://www.mdpi.com/2304-6732/6/4/117/s1, Figure S1: Quantum dot characteristics (absorption spectrum is shown in dashed line; fluorescence spectrum is shown in solid line; the data on QD hydrodynamic diameter distribution are presented in the inset).

**Author Contributions:** Conceptualization—G.N., I.N. and A.S.; Data curation—G.N. and A.S.; Formal analysis—G.N., F.R.G. and A.S.; Investigation—G.N., D.K. and A.S.; Methodology—G.N., D.K., M.B., F.R.G., and A.S.; Supervision—I.N. and A.S.; Visualization—M.B., F.R.G. and F.A.; Writing—original draft—G.N., A.K., I.N. and A.S.; Writing—review & editing—G.N., D.K., A.K., I.N., and A.S.

**Funding:** This study was supported by the Ministry of Science and Higher Education of the Russian Federation, State Contract no. 16.1034.2017/ПЧ.

**Acknowledgments:** We thank Pavel Samokhvalov for providing samples of as-synthetized QDs, Vladimir Ushakov for proofreading the manuscript, and Bärbel Heidrich for excellent technical assistance.

**Conflicts of Interest:** The authors declare that the research was conducted in the absence of any commercial or financial relationships that could be construed as a potential conflict of interest.

## References

1. Reisch, A.; Klymchenko, A.S. Fluorescent Polymer Nanoparticles Based on Dyes: Seeking Brighter Tools for Bioimaging. *Small* **2016**, *12*, 1968–1992. [CrossRef]
2. Hou, J.T.; Ren, W.X.; Li, K.; Seo, J.; Sharma, A.; Yu, X.Q.; Kim, J.S. Fluorescent bioimaging of pH: From design to applications. *Chem. Soc. Rev.* **2017**, *46*, 2076–2090. [CrossRef] [PubMed]
3. Martynenko, I.V.; Litvin, A.P.; Purcell-Milton, F.; Baranov, A.V.; Fedorov, A.V.; Gun'Ko, Y.K. Application of semiconductor quantum dots in bioimaging and biosensing. *J. Mater. Chem. B* **2017**, *5*, 6701–6727. [CrossRef]
4. Resch-Genger, U.; Grabolle, M.; Cavaliere-Jaricot, S.; Nitschke, R.; Nann, T. Quantum dots versus organic dyes as fluorescent labels. *Nat. Methods* **2008**, *5*, 763–775. [CrossRef] [PubMed]
5. Bilan, R.; Nabiev, I.; Sukhanova, A. Quantum dot-based nanotools for bioimaging, diagnostics, and drug delivery. *ChemBioChem* **2016**, *17*, 2103–2114. [CrossRef] [PubMed]
6. Romoser, A.; Ritter, D.; Majitha, R.; Meissner, K.E.; McShane, M.; Sayes, C.M. Mitigation of quantum dot cytotoxicity by microencapsulation. *PLoS ONE* **2011**, *6*, e22079. [CrossRef] [PubMed]
7. Peng, H.; Chiu, D.T. Soft fluorescent nanomaterials for biological and biomedical imaging. *Chem. Soc. Rev.* **2015**, *44*, 4699–4722. [CrossRef]
8. Bilan, R.; Ametzazurra, A.; Brazhnik, K.; Escorza, S.; Fernández, D.; Uríbarri, M.; Nabiev, I.; Sukhanova, A. Quantum-dot-based suspension microarray for multiplex detection of lung cancer markers: Preclinical validation and comparison with the Luminex xMAP® system. *Sci. Rep.* **2017**, *7*, 44668. [CrossRef]
9. Chen, J.; Ratnayaka, S.; Alford, A.; Kozlovskaya, V.; Liu, F.; Xue, B.; Hoyt, K.; Kharlampieva, E. Theranostic Multilayer Capsules for Ultrasound. *ACS Nano* **2017**, *11*, 3135–3146. [CrossRef]
10. Wang, L.; Björnmalm, M.; Hao, J.; Cui, J. Nanoengineering of Soft Polymer Particles for Exploring Bio-Nano Interactions. In *Handbook of Nanomaterials for Cancer Theranostics*; Conde, J., Ed.; Elsevier: Amsterdam, The Netherlands, 2018; pp. 393–419, ISBN 978-0-12-813339-2.
11. Johnston, A.P.R.; Kamphuis, M.M.J.; Such, G.K.; Scott, A.M.; Nice, E.C.; Heath, J.K.; Caruso, F. Targeting cancer cells: Controlling the binding and internalization of antibody-functionalized capsules. *ACS Nano* **2012**, *6*, 6667–6674. [CrossRef]
12. Nifontova, G.; Baryshnikova, M.; Ramos-Gomes, F.; Alves, F.; Nabiev, I.; Sukhanova, A. Engineering of fluorescent biomaging tools for cancer cell targeting based on polyelectrolyte microcapsules encoded with quantum dots. In Proceedings of the 4th International Conference on Applications of Optics and Photonics, AOP2019, Lisbon, Portugal, 31 May–1 June 2019; SPIE: Bellingham, WA, USA, 2019; pp. 1–6.

13. Ohnaga, T.; Takei, Y.; Nagata, T.; Shimada, Y. Highly Efficient Capture of Cancer Cells Expressing EGFR by Microfluidic Methods Based on Antigen-Antibody Association. *Sci. Rep.* **2018**, *8*, 12005. [CrossRef] [PubMed]
14. Sigismund, S.; Avanzato, D.; Lanzetti, L. Emerging functions of the EGFR in cancer. *Mol. Oncol.* **2018**, *12*, 3–20. [CrossRef] [PubMed]
15. Nicholson, R.I.; Gee, J.M.W.; Harper, M.E. EGFR and Cancer Prognosis. *Eur. J. Cancer* **2001**, *37*, 9–15. [CrossRef]
16. Brazhnik, K.; Sokolova, Z.; Baryshnikova, M.; Bilan, R.; Efimov, A.; Nabiev, I.; Sukhanova, A. Quantum dot-based lab-on-a-bead system for multiplexed detection of free and total prostate-specific antigens in clinical human serum samples. *Nanomed. Nanotechnol. Biol. Med.* **2015**, *11*, 1065–1075. [CrossRef]
17. Nifontova, G.; Zvaigzne, M.; Baryshnikova, M.; Korostylev, E.; Ramos-Gomes, F.; Alves, F.; Nabiev, I.; Sukhanova, A. Next-Generation Theranostic Agents Based on Polyelectrolyte Microcapsules Encoded with Semiconductor Nanocrystals: Development and Functional Characterization. *Nanoscale Res. Lett.* **2018**, *13*, 30. [CrossRef]
18. Nifontova, G.; Efimov, A.; Agapova, O.; Agapov, I.; Nabiev, I.; Sukhanova, A. Bioimaging Tools Based on Polyelectrolyte Microcapsules Encoded with Fluorescent Semiconductor Nanoparticles: Design and Characterization of the Fluorescent Properties. *Nanoscale Res. Lett.* **2019**, *14*, 29. [CrossRef]
19. Nifontova, G.; Ramos-Gomes, F.; Baryshnikova, M.; Alves, F.; Nabiev, I.; Sukhanova, A. Cancer Cell Targeting With Functionalized Quantum Dot-Encoded Polyelectrolyte Microcapsules. *Front. Chem.* **2019**, *7*, 34. [CrossRef]
20. Sukhorukov, G.B.; Volodkin, D.V.; Günther, A.M.; Petrov, A.I.; Shenoy, D.B.; Möhwald, H. Porous calcium carbonate microparticles as templates for encapsulation of bioactive compounds. *J. Mater. Chem.* **2004**, *14*, 2073–2081. [CrossRef]
21. Zhang, Y.; Gazit, Z.; Pelled, G.; Gazit, D.; Vunjak-Novakovic, G. Patterning osteogenesis by inducible gene expression in microfluidic culture systems. *Integr. Biol. (Camb.)* **2011**, *3*, 39–47. [CrossRef]
22. Mihai, M.; Schwarz, S.; Doroftei, F.; Simionescu, B.C. Calcium Carbonate/Polymers Microparticles Tuned by Complementary Polyelectrolytes as Complex Macromolecular Templates. *Cryst. Growth Des.* **2014**, *14*, 6073–6083. [CrossRef]
23. Kastl, L.; Sasse, D.; Wulf, V.; Hartmann, R.; Mircheski, J.; Ranke, C.; Carregal-Romero, S.; Martínez-López, J.A.; Fernández-Chacón, R.; Parak, W.J.; et al. Multiple internalization pathways of polyelectrolyte multilayer capsules into mammalian cells. *ACS Nano* **2013**, *7*, 6605–6618. [CrossRef] [PubMed]